A Quad-Band Antenna with AMC Reflector for WLAN and WiMAX Applications

Ernst W. Coetzee, Johann W. Odendaal, and Johan Joubert

Department of Electrical, Electronic & Computer Engineering
University of Pretoria, Gauteng, 0028, South Africa
u13014422@tuks.co.za

Abstract ─ This letter presents a quad-band antenna with high gain for wireless local area network (WLAN) and Worldwide Interoperability for Microwave Access (WiMAX) communication covering the IEEE 802.11a/b and IEEE802.16d/e standards. The antenna consists of a microstrip feed line with a complementary microstrip-slot pair and a secondary slot element on a single dielectric medium. A single-band artificial magnetic conductor (AMC) surface was used as a reflector to achieve a unidirectional radiation pattern with an average gain of 9.3 dBi. The antenna was optimized to achieve a radiation efficiency of more than 90% in the WLAN and WiMAX frequency bands. The size of the antenna with the AMC reflector is 80×80×10 mm^3. The radiation properties of the antenna were measured in a compact antenna range and simulated and measured results are presented.

Index Terms ─ AMC, directional antennas, multi-band antenna, wireless local area network (WLAN), Worldwide Interoperability for Microwave Access (WiMAX).

I. INTRODUCTION

The design of a multi-band, high-gain, low-profile and directional antenna for wireless local area network (WLAN) applications have become more desirable in communication solutions [1]. The WLAN frequency bands include 2.4 – 2.483, 5.15 – 5.25 and 5.725 – 5.825 GHz for the IEEE802.11a/b standards.

The application of artificial magnetic conductor (AMC) surfaces have become more popular in antenna applications, due to improved antenna performance and low-profile designs [2]. Various antennas with AMC reflectors suitable for WLAN applications were proposed and include a dual-band C-slotted, a wideband circularly polarized antenna, a circular disc monopole, and a V-shaped slot antenna. These antennas all have an average gain of less than 8.0 dBi in the WLAN frequency bands or are larger than 80×80×11 mm^3.

A dual-band C-slotted antenna with a single-band diamond shaped AMC reflector is presented in [3]. The antenna had an overall size of 90×90×6.5 mm^3, which was larger than 80×80×11 mm^3. The antenna operated in the 2.4 and 5.8 GHz WLAN frequency bands with gains of about 5.3 and 10.7 dBi.

A wideband circularly polarized antenna with a single-band patch AMC reflector was proposed in [4]. The antenna consisted of two barbed-shape dipoles and two bowtie dipoles printed on the same substrate. The AMC reflector, 80×80 mm^2, was positioned at 17 mm from the antenna substrate and had peak gains of 6.6 and 7.4 dBi in the 2.4 and 5 GHz WLAN frequency bands.

A wideband circular disc monopole antenna was combined with a dual-band AMC reflector, as proposed in [5]. The combination of the wideband monopole antenna with a dual-band AMC resulted in a dual-band response which covered the 2.4 and 5 GHz WLAN bands. The antenna had a size of 88×88×7.8 mm^3 and gains of 3.9 and 6 dBi in the 2.4 and 5 GHz bands.

The combination of a dual-band V-shaped slot etched monopole antenna with a dual-band AMC surface was proposed in [6]. The antenna had a size of 57×57×12.68 mm^3 and due to the monopole antenna, the peak gains were 6.6 and 7.8 dBi at 2.4 and 5.5 GHz.

The proposed quad-band antenna is based on an ultra-wideband slot radiating element presented in [7]. The ultra-wideband characteristics of the strip-slot pair were implemented in [8], where the feedline was terminated with a short circuit termination. The antenna was combined with a perfect electric conductor (PEC) reflector, which resulted in a high-gain directional antenna for WLAN and WiMAX applications.

In this letter, a new high-gain antenna that operates in the IEEE802.11a/b WLAN frequency bands is presented. The PEC reflector is replaced with an AMC reflector and an additional slot element is included. The antenna is combined with a single-band AMC reflector and has an overall size of 80×80×10 mm^3 with measured gains of 9.6, 8.6 and 10.3 dBi in the three WLAN frequency bands. The antenna is also suitable for Worldwide Interoperability for Microwave Access (WiMAX) applications in the frequency band 3.4 – 3.6 GHz [9].

Submitted On: September 29, 2018
Accepted On: October 1, 2018

II. ANTENNA DESIGN

The geometry of the proposed quad-band antenna is shown in Fig. 1.

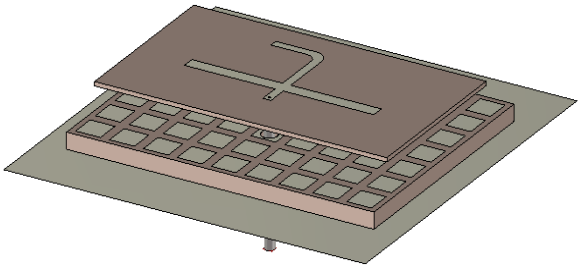

Fig. 1. 3D view of the proposed quad-band antenna.

The slot radiating element structure consists of a microstrip line with a microstrip stub and a complementary slot in the ground plane, which is approximately the same size as the microstrip stub. The combination of the microstrip-slot pair results in an even- and odd-mode and the analysis of it was performed in [7]. he modes are referred to as quasi-strip and quasi-slot modes and the even- and odd-modes can be approximated by [7]

$$Z_{0e} \approx 2Z_M, \quad \epsilon_{eff,e} \approx \epsilon_{eff,M}\,, \tag{1}$$

$$Z_{0o} \approx \frac{Z_S}{2}, \quad \epsilon_{eff,o} \approx \epsilon_{eff,S}\,, \tag{2}$$

where Z_{0e} and Z_{0o} signify the characteristic impedances for the even- and odd-modes of the substructure. The characteristic impedances of the microstrip line and the slot are presented by Z_M and Z_S, respectively. The effective dielectric constant for the even-mode, $\epsilon_{eff,e}$, is equal to the effective dielectric constant of the microstrip line, $\epsilon_{eff,M}$. The effective dielectric constant for the odd-mode, $\epsilon_{eff,o}$, is also equal to the effective dielectric constant for the slot, $\epsilon_{eff,S}$. The image impedance of the microstrip-slot pair is then determined by [7]:

$$Z_{im} = \sqrt{Z_{0e}.Z_{0o}.\cot\theta_e\,.\tan\theta_o}\,, \tag{3}$$

where θ_e and θ_o are the electrical lengths of the even- and odd-modes, respectively. When the effect of losses is ignored, the electrical lengths can be approximated in terms of transmission line parameters as [7]:

$$\theta_e = \sqrt{\epsilon_{eff,M}} \times L_M\,, \tag{4}$$

$$\theta_o = \sqrt{\epsilon_{eff,S}} \times L_{S1}\,, \tag{5}$$

where L_M is the length of the microstrip line, when measured from the microstrip feed line and L_{S1} is the length of the slot when measured from the centre of the slot. When the electrical lengths of both modes are made equal to each other ($\theta_e = \theta_o$), the characteristic impedance of the microstrip feedline can be calculated as [7]:

$$Z_0 = \frac{1}{2}\sqrt{Z_{0e}.Z_{0o}}\,, \tag{6}$$

which is also used as a design condition to achieve impedance matching. The microstrip-slot pair structure can be described by four parameters W_M, W_{S1}, L_M and L_{S1}, which are the widths and lengths of the microstrip line stub and the slot.

An additional slot element was also incorporated to increase the bandwidth. The size of the secondary slot element is almost half the size of the initial slot and was placed close to the initial slot. This resulted in an additional resonance close to the resonance created by the strip-slot pair and improved the impedance bandwidth of the antenna.

The feedline of the proposed antenna was terminated with an open circuit, which improved the radiation efficiency to above 90% in the frequency bands of operation. The dimensions of the antenna structure are shown in Fig. 2 and summarized in Table 1. The antenna was designed on 0.81 mm thick Rogers RO4003C with a dielectric constant of 3.38 and a loss tangent of 0.0027. The antenna is fed with a 50Ω coaxial transmission line through the back of the AMC reflector.

The AMC reflector has a size of 80×80×3.2 mm^3. The spacing between the antenna and AMC was 6 mm and optimized for improved impedance bandwidth. The AMC reflector is printed on 3.2 mm thick FR4 substrate with a dielectric constant of 4.4 and a loss tangent of 0.02. The AMC consists of an array of rectangular patches, where the size of a unit cell is 7.5 mm and the size of the patch is 5.5 mm. The AMC reflector has a 0° reflection phase at 5.6 GHz, with a ±45° reflection phase bandwidth of 4.8 – 6.1 GHz (23.9%), which covers the 5.2 and 5.8 GHZ WLAN bands.

The near electric fields close to the antenna are shown in Fig. 3 at the respective resonances. The lower operating resonance at 2.4 GHz is primarily controlled by the length of the antenna substrate/ground (L). The AMC surface and the ground plane of the antenna support a radiating patch mode, as can be seen by the high value fields in Fig. 3 (a) at the two vertical edges of the antenna ground plane. Design equations of a patch antenna can be implemented to determine the size of the antenna substrate/ground. Figure 3 (b) shows that the resonance at 3.5 GHz is achieved by the unique coupling between the strip-slot pair and the secondary slot element.

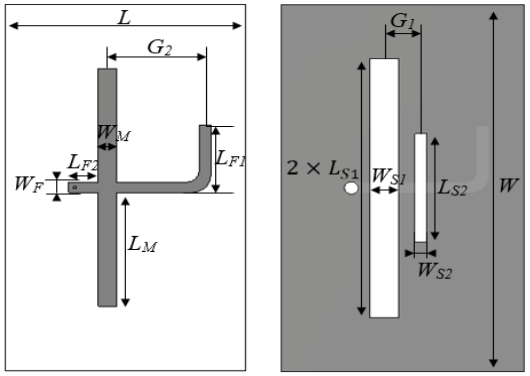

Fig. 2. Layout and dimensions of the quad-band antenna: (a) top and (b) bottom.

Table 1: Dimensions of quad-band antenna

Dimension	Length (mm)	Parameter
L	37.50	Substrate length
W	64.74	Substrate width
$2\times L_{S1}$	45.72	Slot length
W_{S1}	4.43	Slot width
L_{S2}	19.11	Secondary slot length
W_{S2}	1.79	Secondary slot width
G_1	5.59	Gap between slots
L_M	20.08	Strip length
W_M	2.82	Strip width
G_2	15.19	Gap length
L_{F1}	11.90	Curve Length
L_{F2}	4.62	Feed line length
W_F	1.80	Feed line width

The antenna achieves two resonances in the upper operating WLAN band, which allows for the 5.2 and 5.8 GHz WLAN bands to be covered. The upper operating frequency band is controlled by the length of the strip-slot pair (dimension L_M and L_{S1}) as well as the length of the secondary slot element (dimension L_{S2}). Figure 3 (d) shows that 5.8 GHz resonance is controlled by the length of the strip-slot pair and can be determined by implementing equation (1) to (6). Figure 3 (c) shows that the 5.2 GHz resonance is controlled by the length of the secondary slot element. The length of the secondary slot element, L_{S2}, can be determined by first calculating the effective dielectric constant of the slot, ϵ_a, from equation (7). Thereafter the length of the secondary slot element, L_{S2}, is determined from equation (8). This slot is half a wavelength long which indicates that the secondary slot element operates at a half wavelength in the slot:

$$\epsilon_a = \frac{\epsilon_r + 1}{2}, \tag{7}$$

$$L_{S2} = \frac{c}{2f_c\sqrt{\epsilon_a}}. \tag{8}$$

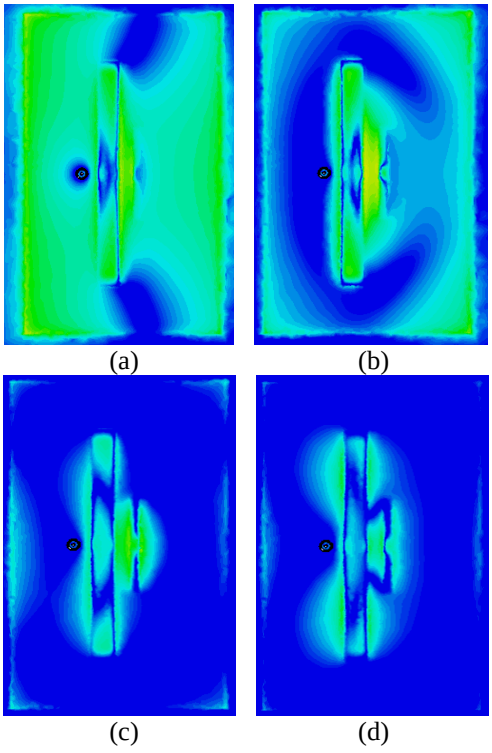

Fig. 3. Electromagnetic field intensity close to the antenna: (a) 2.4 GHz, (b) 3.5 GHz, (c) 5.2 GHz, and (d) 5.8 GHz

The antenna is designed on Rogers RO4003C, which has a dielectric constant of 3.38. From equation (7) the effective dielectric constant for the slot, ϵ_a, is calculated to be 2.19. The length of the secondary slot element, L_{S2}, is then calculated to operate at f_c = 5.2 GHz and from equation (8) found to be 19.49 mm.

To ensure that functionality is maintained in one frequency band, the dimension for the other frequency bands can only be adjusted by 10%. The ground plane of the antenna and the AMC reflector acts as a patch antenna and produces the 2.4 GHz resonance, while the AMC was designed to operate at a fixed spacing of 6 mm for the 5.2 and 5.8 GHz resonances. Increasing the spacing between the antenna and the AMC reflector improves the bandwidth of the 2.4 GHz resonance, due to the patch mode, but decreases the bandwidth in the 5.2 and 5.8 GHz resonance as the AMC was designed to operate at 6 mm. The overall size of the AMC reflector has to be larger than the antenna substrate, but the antenna performance is more dependent on the length of the reflector than the width.

III. NUMERICAL MODEL

CST Microwave Studio was used to analyse and design the antenna [10]. The simulation tool allows for two different solvers to be used. The Finite Integration Technique (FIT) based Time Domain Solver (TDS) and the Finite-Element Method (FEM) based Frequency

Domain Solver (FDS). The AMC reflector was simulated with the FDS using a tetrahedral mesh. The design for the AMC reflector, followed the procedure described in [2]. The performance of an infinite repetition of the basic unit cell was simulated, by applying the proper boundary conditions. The boundaries normal the polarization of the incident field was chosen as perfect electric boundaries, while the planes parallel to the polarization of the incident field was chosen as perfect magnetic boundaries. The AMC unit cell with the proper boundary conditions is shown in Fig. 4. The AMC reflector was designed to operate 6 mm away from the antenna. The unit cell was excited with a waveguide port, 6 mm from the top of the unit cell. The AMC reflector consists of a conductor backed dielectric substrate with an array of square conducting patches.

The AMC reflector was combined with the antenna and was also solved with the FDS with a tetrahedral mesh. The antenna was excited with a coaxial transmission line, through the AMC and connected to the microstrip feedline on the top of the antenna. The coaxial feed line was excited with a waveguide port. The antenna was simulated from 2 – 7 GHz with local mesh refinement, while adaptive meshing was applied at the centre frequency of the simulation, at 4.5 GHz. A total of 113234 tetrahedrons were used to provide a sufficient representation of the antenna geometry. The mesh view of the antenna with the tetrahedral meshing is shown in Fig. 5.

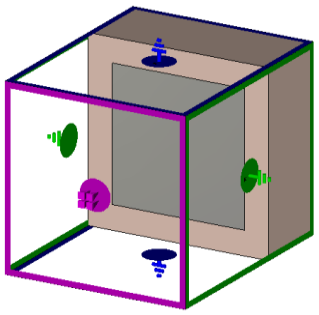

Fig. 4. 3D view of AMC unit cell with boundary conditions.

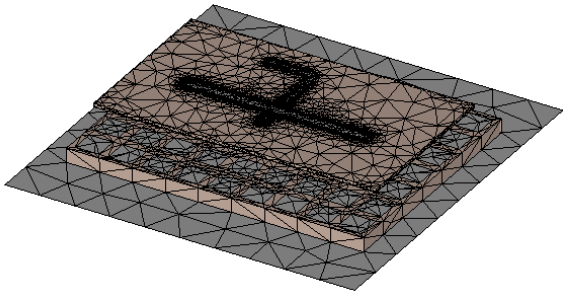

Fig. 5. 3D view of antenna with tetrahedral meshing.

IV. SIMULATIONS AND MEASUREMENTS

The antenna was designed and simulated with CST Microwave Studio. The reflection coefficient of the manufactured antenna was measured with an HP8510 Vector Network Analyzer and the simulated and measured reflection coefficients are shown in Fig. 6. The antenna has a reflection coefficient below -10 dB in all three WLAN frequency bands, as well as the WiMAX bands.

The gain and radiation patterns of the manufactured quad-band antenna were measured in the compact antenna range at the University of Pretoria, as shown in Fig. 7. The simulated realized gain of the antenna is compared to the measured gain in Fig. 8, and the largest difference was found to be 1.7 dBi. The measured average gain was 9.5, 8.6 and 10.2 dBi in the three WLAN bands respectively, and 8.9 dBi in the WiMAX frequency band. The difference between the simulated and measured gain values are likely due to the measurement setup in the compact range. The simulated and measured radiation patterns in the *E*- and *H*-planes at 2.4, 3.5, 5.2 and 5.775 GHz are compared to each other and shown in Fig. 9.

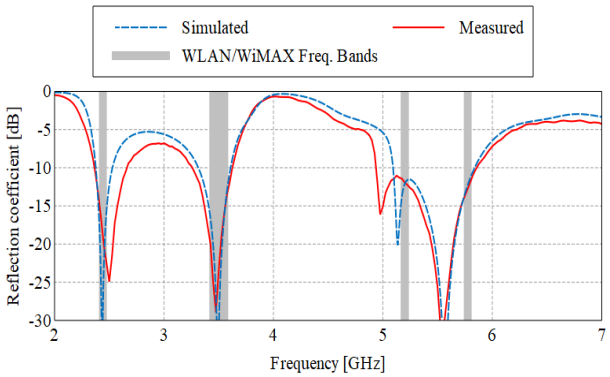

Fig. 6. Simulated and measured reflection coefficient of the antenna.

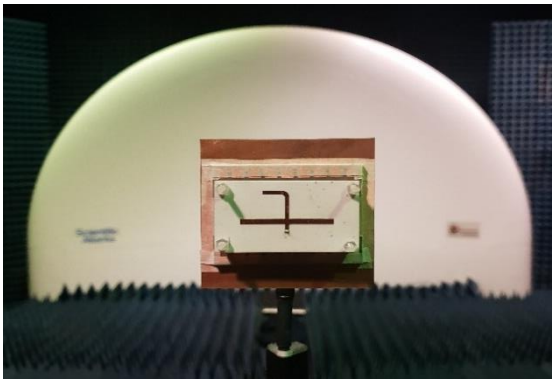

Fig. 7. Manufactured quad-band antenna in the compact antenna range.

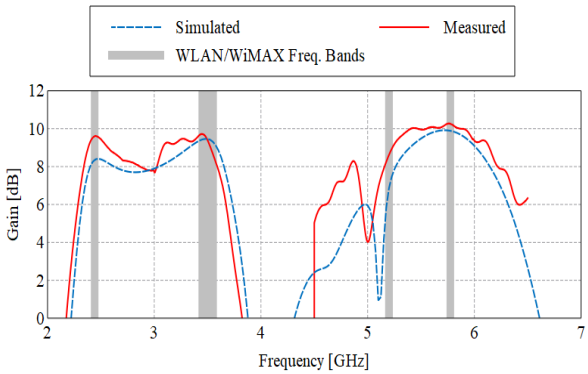

Fig. 8. Simulated and measured gain of the antenna.

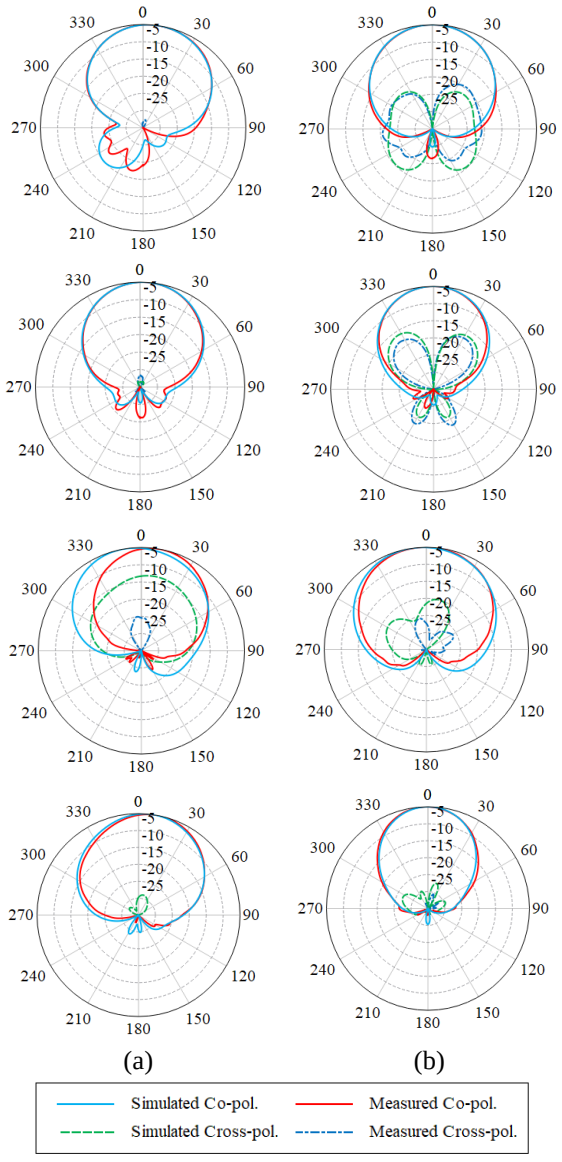

Fig. 9. Simulated and measured radiation patterns in the *E*- and *H*-planes of the antenna at the four frequencies 2.4, 3.5, 5.2 and 5.775 GHz: (a) E-plane and (b) H-plane.

The simulated *E*-plane radiation pattern at 5.2 GHz is slightly wider than the measured pattern. This is the cause for the noticeable difference in gain at 5.2 GHz. The beamwidth at 5.2 GHz is also wider than the beamwidth at 5.775 GHz, which is due to radiation from the secondary slot element. The simulated and measured radiation patterns show good correlation. The measured maximum cross-polarization is less than -20 dB in the E-plane. The front-to-back ratio is also better than -22 dB in the respective WLAN and WiMAX frequency bands.

V. CONCLUSION

The design of a quad-band, high-gain and directional antenna with a low-profile suitable for WLAN and WiMAX applications was presented. The proposed antenna consists of a microstrip-slot pair with a parasitic slot element, to ensure a wide impedance bandwidth. A high radiation efficiency was achieved by terminating the feed line with an optimized open circuit termination. A low-profile design was realized by including an AMC reflector to achieve a directional radiation pattern and high gain. The proposed antenna has a higher gain and smaller size when compared to other directional WLAN antennas found in the literature. The simulated and measured results were compared and have a good correlation.

ACKNOWLEDGMENT

This work is based on research supported by the National Research Foundation (NRF) of South Africa (Grant Number 114941).

REFERENCES

[1] B. Kelothu, K. R. Subhashini, and G. L. Manohar, "A compact high-gain microstrip patch antenna for dual band WLAN applications," *2012 Students Conference on Engineering and Systems*, Allahabad, Uttar Pradesh, pp. 1-5, 2012.

[2] J. Joubert, J. C. Vardaxoglou, W. G. Whittow, and J. W. Odendaal, "CPW-fed cavity-backed slot radiator loaded with an AMC reflector," in *IEEE Transactions on Antennas and Propagation*, vol. 60, no. 2, pp. 735-742, Feb. 2012.

[3] P. J. Soh, F. N. Giman, M. F. Jamlos, H. Lago, and A. A. Al-Hadi, "A C-slotted dual band textile antenna for WBAN applications," *2016 URSI Asia-Pacific Radio Science Conference (URSI AP-RASC)*, Seoul, pp. 1621-1624, 2016.

[4] H. H. Tran and I. Park, "A dual-wideband circularly polarized antenna using an artificial magnetic conductor," in *IEEE Antennas and Wireless Propagation Letters*, vol. 15, pp. 950-953, 2016.

[5] N. A. Abbasi and R. J. Langley, "Multiband-integrated antenna/artificial magnetic conductor," in *IET Microwaves, Antennas & Propagation*, vol.

5, no. 6, pp. 711-717, 26 Apr. 2011.

[6] V. K. Pandit and A. R. Harish, "Design of dual-band CPW-fed monopole antenna with dual-band AMC surface for WLAN," *2016 IEEE Annual India Conference (INDICON)*, Bangalore, pp. 1-4, 2016.

[7] F. Rashid, M. M. Mustafiz, M. K. Ghosh, and S. Hossain, "Design and performance analysis of ultra-wideband inverted-F antenna for Wi-Fi, WiMAX, WLAN and military applications," *2012 15th International Conference on Computer and Information Technology (ICCIT)*, Chittagong, pp. 610-614, 2012.

[8] E. Abdo-Sanchez, J. E. Page, T. M. Martin-Guerrero, J. Esteban, and C. Camacho-Penalosa, "Planar broadband slot radiating element based on microstrip-slot coupling for series-fed arrays," in *IEEE Transactions on Antennas and Propagation*, vol. 60, no. 12, pp. 6037-6042, Dec. 2012.

[9] M. van Rooyen, J. W. Odendaal, and J. Joubert, "High-gain directional antenna for WLAN and WiMAX applications," in *IEEE Antennas and Wireless Propagation Letters*, vol. 16, pp. 286-289, 2017.

[10] CST STUDIO SUITE® 2018, CST AG, Germany, www.cst.com

Ernst W. Coetzee received the B.Eng. and B.Eng.Hons. in Electronic Engineering from the University of Pretoria, Pretoria, South Africa in 2016 and 2017, respectively. He is currently employed as an Assistant Lecturer at the University of Pretoria and also busy with his M.Eng. in Electronic Engineering in the field of electromagnetism.

Johann W. Odendaal (M'90–SM'00) received the B.Eng., M.Eng., and Ph.D. degrees in Electronic Engineering from the University of Pretoria, Pretoria, South Africa, in 1988, 1990, and 1993, respectively. From September 1993 to April 1994, he was a Visiting Scientist with the ElectroScience Laboratory at the Ohio State University. From August to December 2002, he was a Visiting Scientist with CSIRO Telecommunications and Industrial Physics in Australia. Since May 1994, he has been with the University of Pretoria, where he is currently a Full Professor. His research interests include electromagnetic scattering and radiation, compact range measurements, and signal processing. He is also Director of the Centre for Electromagnetism at the University of Pretoria. Odendaal is a Member of the Antenna Measurement Techniques Association (AMTA) and is registered as a Professional Engineer in South Africa

Johan Joubert (M'86–SM'05) received the B.Eng, M.Eng and Ph.D degrees in Electronic Engineering from the University of Pretoria, Pretoria, South Africa, in 1983, 1987 and 1991 respectively. From 1984 to 1988 he was employed as a Research Engineer at the Council for Scientific and Industrial Research, Pretoria. In 1988 he joined the Department of Electrical and Electronic Engineering at the University of Pretoria, where he is currently a Professor of Electromagnetism. From July to December 1995 he was Visiting Scholar with the Department of Electrical and Computer Engineering, California State University, Northridge, USA. From July to December 2001 he was Visiting Scientist at Industrial Research Laboratories in Wellington, New Zealand. From July to December 2006 he was Visiting Scholar at the Institut für Höchstfrequenztechnik und Elektronik, Universität Karlsruhe (TH), Germany, and from July to September 2010 he visited Loughborough University in the UK for a collaborative research project on meta-materials. His research interests include antenna array design and computational electromagnetism. Joubert is a registered Professional Engineer in South Africa.